ORAL/POSTER REFERENCE: ICF100916OR

MODELLING OF SIZE EFFECTS ON FRACTURE IN THE BRITTLE-TO-DUCTILE TRANSITION REGIME

A H Sherry[1], D P G Lidbury[1], D C Connors[2] and A R Dowling[2]

[1]AEA Technology plc, Risley, Warrington, WA3 6AT, UK
[2]BNFL Magnox Generation, Berkeley, Gloucestershire, GL13 9PB, United Kingdom

ABSTRACT

Measurements of toughness in the ductile-to-brittle fracture regime exhibit an effect of test-piece size. For a given level of toughness (K_{JC}), this may be considered as a positive shift in the transition temperature (ΔT) with increasing specimen thickness for a particular geometry. This Paper describes a numerical programme undertaken to investigate the influence of specimen size on the fracture toughness behaviour of submerged-arc weld material in the ductile-to-brittle transition regime. The influences of sampling volume and constraint on ΔT have been assessed for 10 mm thick CT (CT-10) and 20 % side-grooved pre-cracked Charpy specimens (PC-CVN) relative to 25 mm thick standard plane-sided compact-tension (CT-25) specimens. Three-dimensional, elastic-plastic finite element analyses have been used to assess the constraint behaviour of these specimens, and the BEREMIN model has been applied to predict ΔT. The analyses have indicated a loss of constraint over a significant proportion of the crack front for both CT-10 and PC-CVN specimens at toughness levels greater than approximately 100 MPa$\sqrt{m}$. For CT-10 specimens, constraint-loss is most significant towards the outer edges of the specimen whilst high constraint conditions are initially maintained over the central region of the crack-front. This high constraint region may be viewed as an effective crack-front width that reduces with increasing deformation. For side-grooved PC-CVN specimens, constraint loss occurs uniformly across the crack front. Statistical models, based on empirical data, give a value of ΔT = 18 ºC for this material at a mean reference toughness of 100 MPa$\sqrt{m}$. The BEREMIN model tends to over-predict this value by ~ 35 ºC for CT-10 specimens and ~ 55 ºC for side-grooved PC-CVN specimens.

KEY WORDS

Fracture toughness, constraint, size effect, Local Approach

INTRODUCTION

Fracture toughness measurements made within the ductile-to-brittle transition temperature regime are influenced by specimen size. For a given level of toughness, K_{JC}, this may be thought of in terms of a positive shift in the transition temperature, ΔT, with increasing specimen thickness, B. Alternatively, with temperature fixed, the mean toughness derived from tests on small specimens is greater than that obtained from corresponding tests on larger specimens. There are two principal reasons for this size effect.

First, cleavage initiation in ferritic steel is associated with the pile-up of dislocations against brittle second-phase particles. The volume of the crack-tip plastic zone is therefore an important factor in the cleavage process since the greater the volume, the more likely it is that a favourable brittle particle will be sampled. Under LEFM conditions, the volume of the plastic zone is proportional to $K^4 \cdot B$, where K is the stress intensity factor and B is the crack front length (equal to the specimen thickness in standard fracture toughness specimens). The size effect on transition toughness may thus be approximately described by $K_{JC} \propto 1/B^{0.25}$. Statistical models of transition behaviour broadly reflect this scaling relationship:

- Moscovic [2]: $K_{JC} \cdot B^{0.179}$ or $K_{JC} \cdot B^{0.391}$ = constant
- Master Curve [3]: $K_{JC} \cdot B^{0.25}$ = constant

Secondly, the transition between small and large-scale yielding leads to a reduction in crack-tip constraint and a lowering of the hydrostatic stress field. This transition, which leads to an increase in effective toughness, occurs at lower crack driving forces in small compared with large specimens since at the same applied K the radius of the plastic zone is a greater proportion of the uncracked ligament. At a given temperature, constraint loss leads to an increase in the critical value of K required to initiate cleavage. The constraint parameter Q, quantifying the extent to which the actual hydrostatic stress field diverges from that corresponding to small-scale yielding (SSY) conditions, can be defined as [4]:

$$Q = \frac{\sigma_H - (\sigma_H)_{SSY}}{\sigma_0}, \qquad \text{at } \theta = 0, r\sigma_0 / J_z = 2 \tag{1}$$

where r and θ denote polar co-ordinates centred at the crack-tip, J is the J-integral and σ_0 is the yield stress. At low levels of K, the plastic zone is small and Q remains close to zero, but under large-scale yielding, Q becomes negative.

The influences of both sampling volume and constraint loss on cleavage toughness in the transition regime may be simulated using appropriate fracture models. The BEREMIN Local Approach uses a two-parameter Weibull model to describe the influence of crack-tip stress on cleavage probability, p [5]

$$p = 1 - \exp\left\{-\left(\frac{\sigma_W}{\sigma_u}\right)^m\right\} \tag{2}$$

The Weibull stress, σ_W, is defined as a volume integral taken over the fracture process zone, Ω

$$\sigma_W = \left\{ \frac{1}{V_u} \iiint_{\Omega} \sigma_q^m \, d\Omega \right\}^{\frac{1}{m}} \quad (3)$$

The constants, V_u (the characteristic volume), σ_u (the scale parameter) and m (the Weibull modulus) are the parameters of the model. The scalar field, σ_q conventionally represents the distribution of maximum principal stress, σ_1, within the plastic zone.

This Paper describes a numerical programme undertaken to investigate the influences of specimen size (sampling volume and constraint loss) on transition toughness behaviour. In particular, the behaviour of 10 mm thick compact-tension specimens (CT-10) and 20 % side-grooved pre-cracked Charpy specimens (PC-CVN) are assessed relative to standard 25 mm thick compact-tension specimens (CT-25).

MATERIAL

The material of interest is a submerged arc weld (SAW) metal. Tensile properties and BEREMIN parameters are summarised in Table 1, fracture toughness behaviour is illustrated in Fig. 1 [1]. A comparison of the calibrated model with the base-line toughness data is included in Fig. 1.

TABLE 1
TENSILE PROPERTIES AND BEREMIN PARAMETERS FOR SAW MATERIAL

T, ºC	E, GPa	σ_0, MPa	V_u, μm^3	m	σ_u, MPa
-110	216	569	$(50)^3$	13.17	3,733
-70	214	498	$(50)^3$	13.17	3,836
-50	213	470	$(50)^3$	13.17	3,859
-25	211	442	$(50)^3$	13.17	3,877
0	210	419	$(50)^3$	13.17	4,097
25	209	400	$(50)^3$	13.17	4,675

NUMERICAL ANALYSIS

Three-dimensional finite element models of the CT-10 and PC-CVN specimens were developed. Each model consisted of eight-noded full-integration brick elements arranged into planar layers. The thickest layer was towards the centre of the specimen and the thinnest towards the outer surface. In both models, the crack tip was modelled by a series of square-section brick elements of in-plane dimension 50 μm. Figure 2 illustrates the PC-CVN model.

A series of small-strain elastic-plastic finite element analyses were performed with stress-strain data appropriate to fourteen temperatures in the range –150 to +25 ºC. A series of SSY analyses were also performed within the framework of a boundary layer model to simulate the behaviour of a crack in an infinite body under high constraint plane strain conditions. The

crack-tip stress and strain fields derived from these analyses were post-processed to define the variation of Q as a function of increasing load using Eqn. (1), and p as a function of K_J and temperature using Eqns. (2) and (3).

RESULTS

Crack driving force

Figures 3 and 4 illustrate the variation of K_J across the crack front for CT-10 and PC-CVN specimens respectively. Here, the deformation level has been indexed by the parameter M, where $M = b\sigma_0/J$. Here b is the ligament size. M decreases with increasing deformation. Current validity limits in fracture toughness testing require that $M \geq 30$ at cleavage for fracture toughness data to be valid.

For the CT-10 specimen, the peak value of K_J is located at the centre of the specimen and reduces towards the outer surface for all load levels. For the PC-CVN specimen, the peak value of K_J is located at the root of the side-grooves, which act as a stress-concentrating feature. These results are similar to those presented elsewhere for plane and side-grooved specimens [6]. In order to define a crack-tip loading parameter applicable to the full width of the specimen, an average value of K_J ($K_{J,ave}$) has been calculated.

Crack-tip constraint

Figure 5 shows the variation of Q across the CT-10 specimen at different load levels. For low loads, a large proportion of the crack front is under high constraint (here defined as $Q \geq -0.1$), but Q decreases towards the outer surface. As the load level increases, the proportion of the crack front under high constraint reduces. Figure 6 shows similar results for the PC-CVN specimen. Again, at low loads, most of the crack front is under high constraint, but Q decreases slightly towards the root of the side grooves. As loading increases, constraint reduces uniformly across the crack front.

Predicted transition behaviour

Predicted transition curves using Eqns. (2) and (3) and p = 5, 50 and 95 % for CT-10 and PC-CVN specimens are compared with base-line CT-25 data in Figs. 7 and 8 respectively. Also shown are loci of constant M (30 and 80). Relative to the base-line data at 100 MPa√m, the predicted curves for the CT-10 and PC-CVN specimens exhibit a shift of approximately 55 º and 75 ºC respectively. These values are larger than that of 18 ºC derived from statistical analysis of actual data [2]. The model predictions show an increase in scatter compared with the base-line data. At –75 ºC, the base-line data indicate a scatter between the 5^{th} and 95^{th} percentiles of ~ 100 MPa√m, whereas that predicted for the CT-10 and PC-CVN specimens is greater than 200 and 300 MPa√m respectively.

DISCUSSION

The elastic and elastic-plastic stress intensity factor calculations emphasise the three-dimensional nature of deformation in fracture toughness specimens. The Q-stress profiles plotted in Figs. 5 and 6 illustrate the variation of constraint conditions through the thickness of fracture specimens.

For the CT-10 specimen, crack-tip constraint is reduced at the outer surfaces of the specimen at moderate loading levels, Fig. 5. As the loading level increases, the low constraint region progressively extends towards the centre of the specimen until, at M ≈ 30, low constraint conditions dominate across almost the full crack front. This observation leads to two important implications.

Sampling volume: the volume of highly stressed (i.e. high constraint) material ahead of the crack-tip may be smaller than that assumed by the $B^{0.25}$ scaling law, particularly for high load levels. Under these conditions, such scaling laws may under-predict the size effect since they inherently assume high constraint to extends across the full thickness. This observation has led Nevalainen and Dodds [6] to calculate effective specimen thicknesses (B_{eff}) for both CT-10 and plane-sided PC-CVN specimens based on the areas enclosed within the principal stress contour $\sigma_1/\sigma_0 = 3$. For a CT-10 specimen with a work hardening exponent n = 5 to 10, $B_{eff} \approx 0.5B$ for M < 90. This is consistent with the Q-stress data presented in Fig. 5. For a plane-sided PC-CVN specimen, $B_{eff} \approx 0.65B$ for M < 125.

Constraint effects: at fracture, the level of crack-tip constraint across the specimen width may be somewhat less than that under SSY leading to an enhancement in cleavage fracture toughness. To ensure fracture toughness data relate to high constraint conditions across a significant proportion of the crack front width, the results presented in Figs. 5 and 6 suggest that the value of M at fracture should be greater than 100 for CT-10 specimens and greater than 60 for side-grooved PC-CVN specimens.

For the CT-10 and PC-CVN specimens, the Local Approach model predicts significantly higher values of ΔT, by margins of 35 º and 55 ºC, than that derived from the $B^{0.25}$ scaling law. A difference has been observed in using small specimens to measure the Master Curve parameter T_0 [3]. For some materials there appears to be a difference between the value of T_0 derived from tests on 10 mm thick specimens and that for larger specimens. Size-dependent values of T_0 were obtained from specimen data relating to a range of nuclear pressure vessel steels [8]. As the deformation index M decreases the values of T_0 derived from PC-CVN specimens tend to reduce below those obtained from larger specimens. Work by Tregoning [9] shows that this effect may be material dependent and even negligible for some materials. Thus, it is clear that there can be an influence of specimen size different from that predicted by a $B^{0.25}$ scaling law. The Local Approach model results presented in this paper tend to over-predict the magnitude of this difference.

CONCLUSIONS

1. The finite element analyses have indicated a loss of constraint over a significant proportion of the crack front for M < ~100 for CT-10 and M < ~60 for side-grooved PC-CVN specimens.
2. For CT-10 specimens, constraint loss is most significant towards the outer edges of the specimen. High constraint conditions are maintained over the central 50 % of the crack-front for M > 100.
3. For side-grooved PC-CVN specimens, constraint loss occurs uniformly across the crack front. High constraint conditions are maintained over 90 % of the crack front for M > 60.
4. To ensure fracture toughness data relate to high constraint conditions across a significant proportion of the crack front width, the current results suggest that the value of M at

fracture should be greater than 100 for CT-10 specimens and greater than 60 for side-grooved PC-CVN specimens.

5. Statistical models, based on empirical data, give a value of ΔT of 18 ºC at a mean toughness of 100 MPa√m. The BEREMIN model over-predicts this by ~ 35 ºC for CT-10 specimens and 55 ºC for side-grooved PC-CVN specimens.
6. A review of experimental data relating to RPV steel sub-sized specimens has revealed a difference in ΔT values predicted by the $B^{0.25}$ scaling law and those derived from sub-sized specimens. The magnitude of this difference, at a mean toughness level of 100 MPa√m, may be up to 30 ºC for some materials.

ACKNOWLEDGEMENTS

This work was funded by, and is published with the permission of BNFL Magnox Generation. The authors are grateful to Prof. R H Dodds (University of Illinois) and Dr M T Kirk (USNRC) for informal technical discussions during the course of the work.

REFERENCES

[1] A R Dowling and D P G Lidbury, "Local Approach modelling of constraint contributions to the ductile to brittle transition", in *Fracture, Plastic Flow and Structural Integrity*, Proceedings of the 7th Symposium organised by the Technical Advisory Group on Structural Integrity of Nuclear Plant, Eds. P Hirsch and D Lidbury, 2000.

[2] R Moskovic, "Statistical Analysis of censored fracture toughness data in the ductile to brittle transition temperature region", Engng Fract. Mech., Vol. 44, pp. 21-41, 1993.

[3] K Wallin, "Fracture toughness transition curve shape for ferritic structural steels", in *Fracture of Engineering Materials and Structures*, Edited by S T Teoh and K H Lee, Elsevier Applied Science, pp. 83-88, 1991.

[4] N P O'Dowd and C F Shih, "Two-parameter fracture mechanics: theory and application", NUREG/CR-5958, 1993.

[5] F M BEREMIN, "A Local Criterion for Cleavage Fracture of Nuclear Pressure vessel Steels", Metallurgical Transactions, Vol. 14A, pp. 2277-2287, 1983.

[6] M Nevalainen and R H Dodds, "Numerical investigation of 3-D constraint effects on brittle fracture in SE(C) and C(T) specimens", *Int. J. Fract.*, Vol. 74, pp. 131-161, 1995.

[7] J D S Sumpter and J W Hancock, "Status review of the J plus T stress", presented at the 10th European Conference on Fracture, Berlin, 20-23 September 1994.

[8] M T Kirk, private communication, August 2000.

[9] R L Tregoning, "Application of Master Curve approach for design and structural integrity assessment", presented at IG-RDM8 Open Workshop on Fracture Toughness Master Curve for Reactor Pressure Vessel Steels, Nashville, January 22, 1999.

[10] C Ruggieri, R H Dodds and K Wallin, "Constraint effects on reference temperature, T_0, for ferritic steels in the transition region", *Engng Fract. Mech.*, Vol. 60, pp. 19-36, 1998.

[11] M T Kirk and M Mitchell, "A review of technical and regulatory developments needed to enable application of Master Curve technology to the fracture integrity assessment of commercial nuclear power reactors", ASME PVP- Vol. 412, pp. 187-195, 2000.

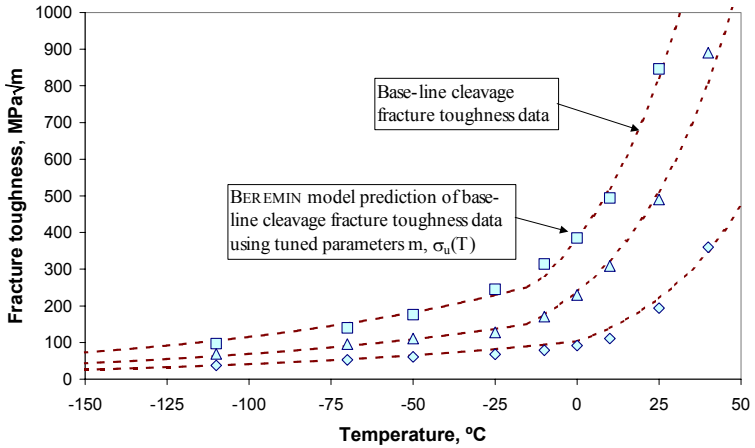

Figure 1:. SAW baseline fracture toughness data for CT-25 specimens. Statistical model and BEREMIN model prediction.

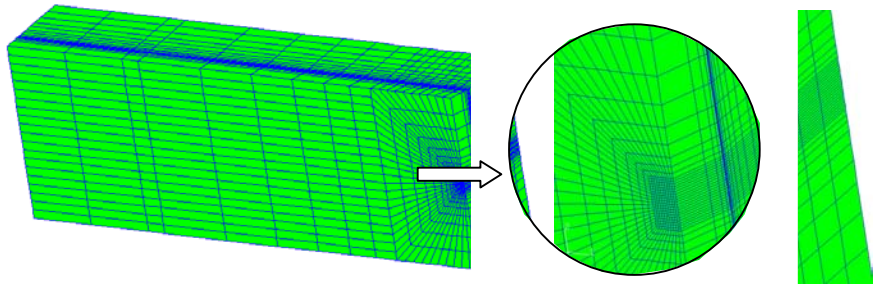

Figure 2: Finite element model of PC-CVN specimen. B = 10mm; W = 10 mm; a/W = 0.5; SG = 20%

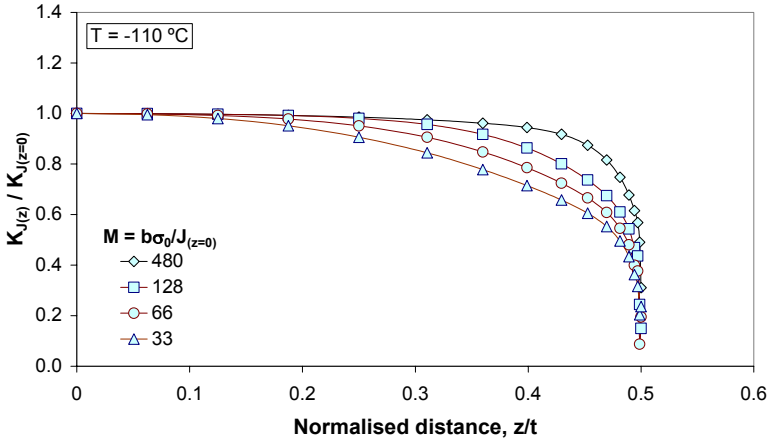

Figure 3: Normalised K_J as a function of distance along the crack front. CT-10 specimen.

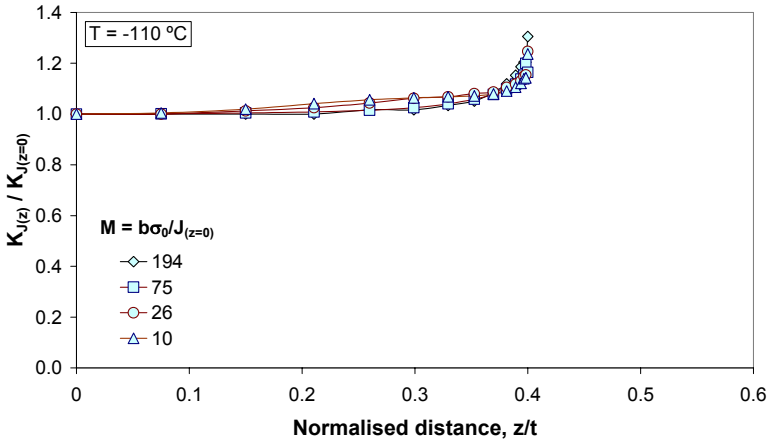

Figure 4: Normalised K_J as a function of distance along the crack front. PC-CVN specimen.

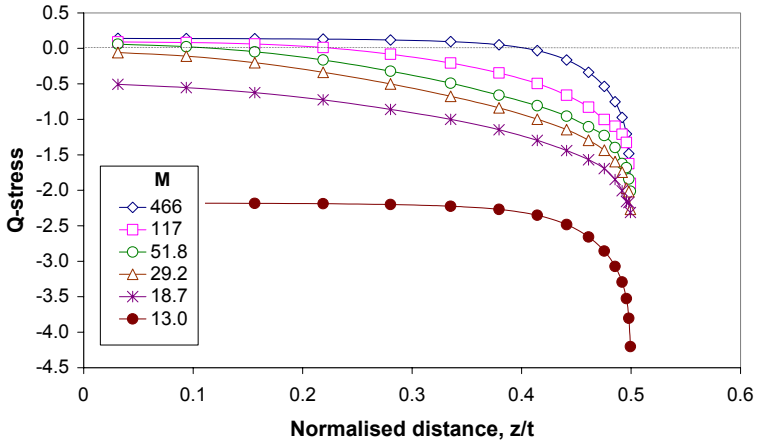

Figure 5: Q as a function of distance along the crack front. CT-10 specimen.

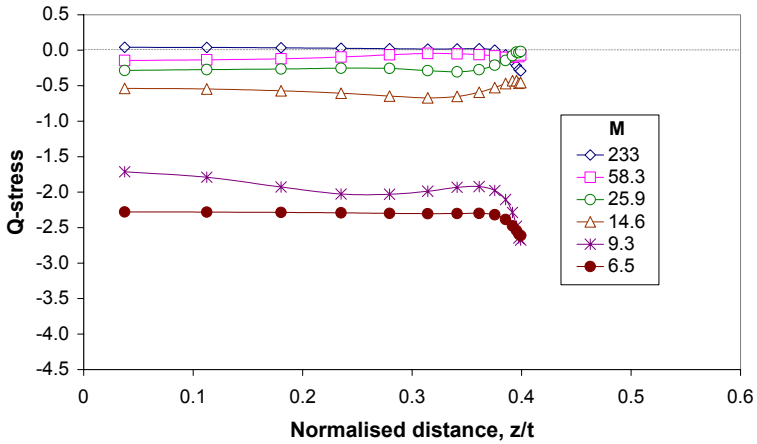

Figure 6: Q as a function of distance along the crack front. PC-CVN specimen.

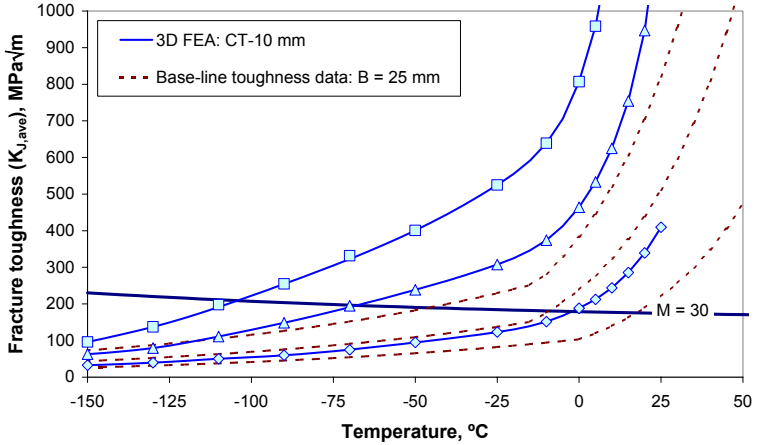

Figure 7: Predicted transition behaviour for CT-10 specimen.

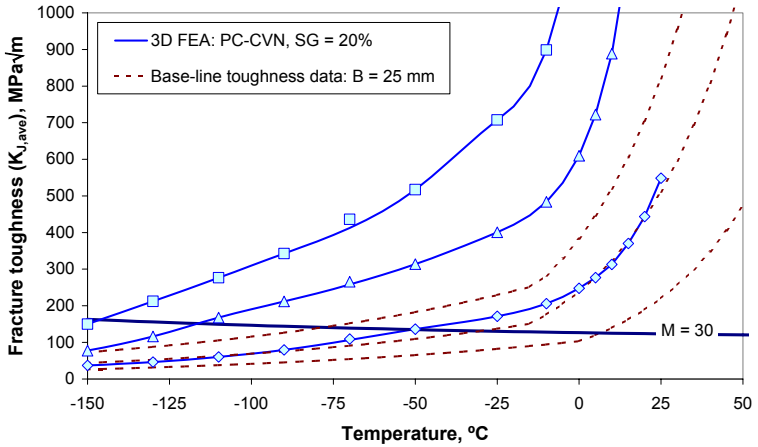

Figure 8: Predicted transition behaviour for PC-CVN specimen.